JVI Journals.ASM.org

Knockout of cGAS and STING Rescues Virus Infection of Plasmid DNA-Transfected Cells

Martijn A. Langereis, Huib H. Rabouw, Melle Holwerda, Linda J. Visser, Frank J. M. van Kuppeveld

Virology Division, Department of Infectious Diseases and Immunology, Faculty of Veterinary Medicine, Utrecht University, Utrecht, The Netherlands

It is well known that plasmid DNA transfection, prior to virus infection, negatively affects infection efficiency. Here, we show that cytosolic plasmid DNA activates the cGAS/STING signaling pathway, which ultimately leads to the induction of an antiviral state of the cells. Using a transient one-plasmid clustered regularly interspaced short palindromic repeat (CRISPR)/Cas9 system, we generated cGAS/STING-knockout cells and show that these cells can be infected after plasmid DNA transfection as efficiently as nontransfected cells.

Mammalian cells express various receptors to sense invading pathogens. Specialized receptors that survey the intracellular milieu are the NOD-like receptors (NLRs), the RIG-I-like receptors (RLRs), and numerous receptors that detect cytosolic DNA (1). Recently, a ubiquitously expressed DNA sensor, cyclic GMP-AMP synthase (cGAS), has been identified (2, 3). Upon binding of cytosolic DNA, like herring testis DNA and poly(dA:dT), cGAS produces cyclic GMP-AMP signaling molecules that subsequently activate stimulator of interferon genes (STING [4, 5]). STING then activates a cascade that results in the synthesis and secretion of type I interferons (interferon alpha/beta [IFN-α/β]), ultimately leading to the induction of an antiviral state of the cells.

Plasmid DNA transfection is often used as a transient gene delivery system to overexpress proteins (e.g., dominant negative or green fluorescent protein [GFP] fusion proteins). Unfortunately, in many cases the transfection procedure blocks virus infection. Although it is conceivable that transfected plasmid DNA activates the cGAS/STING pathway, which might lead to an antiviral state of the cells, this has not been properly investigated.

To study the plasmid DNA-mediated repression of virus infection, we transfected red fluorescent protein (RFP)-encoding plasmid DNA into HeLa-R19 and BGM cells using Fugene 6 (similar experiments, with comparable results, have been performed using Lipofectamine 2000 and JetPRIME [data not shown]). Twenty-four hours posttransfection, the cells were infected with the coxsackievirus B3-enhanced GFP (CVB3-EGFP) and mengovirus-EGFP (mengo-EGFP) reporter viruses, and infection efficiency was monitored using flow cytometry analysis. We observed a marked decrease in CVB3-EGFP infection efficiency in plasmid DNA-transfected HeLa-R19 cells (from 70% to 31%) and BGM cells (from 43% to 11%) compared to mock-treated cells (Fig. 1A). A comparable decrease in infection efficiency was also observed for mengo-EGFP (Fig. 1B). It is important to note that virus infection was hampered in both RFP-positive and RFP-negative cells. This suggests that plasmid DNA transfection induces the secretion of a soluble factor that restricts virus infection, possibly cGAS/STING-induced IFN-α/β. To investigate this, we performed transfection/infection experiments in HEK293T and Vero-E6 cells, which are known to be deficient in cGAS and STING signaling (3, 6) and the production of IFN-α/β (7), respectively. In these cells, plasmid DNA transfection had no effect on reporter virus infection efficiency (Fig. 1A and B). Thus, the restricted virus infection seems to be dependent on cGAS/STING and the production of IFN-α/β. To verify if the plasmid DNA-induced IFN-α/β production is sufficient to induce an antiviral state of the cells, we transfected plasmid DNA into HeLa-R19 and HEK293T cells and used real-time quantitative PCR (RT-qPCR) to determine mRNA levels of several cytokines and known interferon-stimulated genes (ISGs). We observed a significant increase in cytokine and ISG mRNA levels in HeLa-R19 cells but not in HEK293T cells (Fig. 1C). The ISG mRNA levels correlated with an increase in protein expression (Fig. 1D). The lack of increased ISG expression in HEK293T cells was not caused by a general defect in ISG production, as recombinant IFN-α2 (Roferon-A) treatment boosted ISG protein expression (Fig. 1D). Thus, plasmid DNA transfection induces a cGAS/STING-dependent antiviral state of the cells, which might explain the poor infection efficiency.

In an attempt to tackle the hampered infection efficiency of plasmid DNA-transfected HeLa-R19 cells, we set out to generate cGAS/STING-knockout cells using the clustered regularly interspaced short palindromic repeat (CRISPR)/Cas9 system. This tool is based on the prokaryotic "adaptive immune" response (8), which has been adapted to efficiently edit genomic DNA of eukaryotic cells (9). To utilize this tool, we developed a single-plasmid CRISPR/Cas9 approach where the Cas9 enzyme and two genomic RNA (gRNA) molecules are simultaneously expressed (Fig. 2A). Targeting a cellular gene with two gRNA/Cas9 complexes will result, in many cases, in a specific gene fragment deletion (10). To mutate the cGAS and STING genes, two gRNA sequences per gene were designed to delete a 32-bp (cGAS) and 149-bp (STING) fragment just downstream of the translation initiation site (Fig. 2B). After transient transfection of the CRISPR/Cas9 plasmids and 3 days of puromycin selection, the genomic DNA was isolated and tested for cGAS and STING gene integrity

Received 15 July 2015 **Accepted** 19 August 2015

Accepted manuscript posted online 26 August 2015

Citation Langereis MA, Rabouw HH, Holwerda M, Visser LJ, van Kuppeveld FJM. 2015. Knockout of cGAS and STING rescues virus infection of plasmid DNA-transfected cells. J Virol 89:11169–11173. doi:10.1128/JVI.01781-15.

Editor: S. Perlman

Address correspondence to Frank J. M. van Kuppeveld, F.J.M.vanKuppeveld@uu.nl.

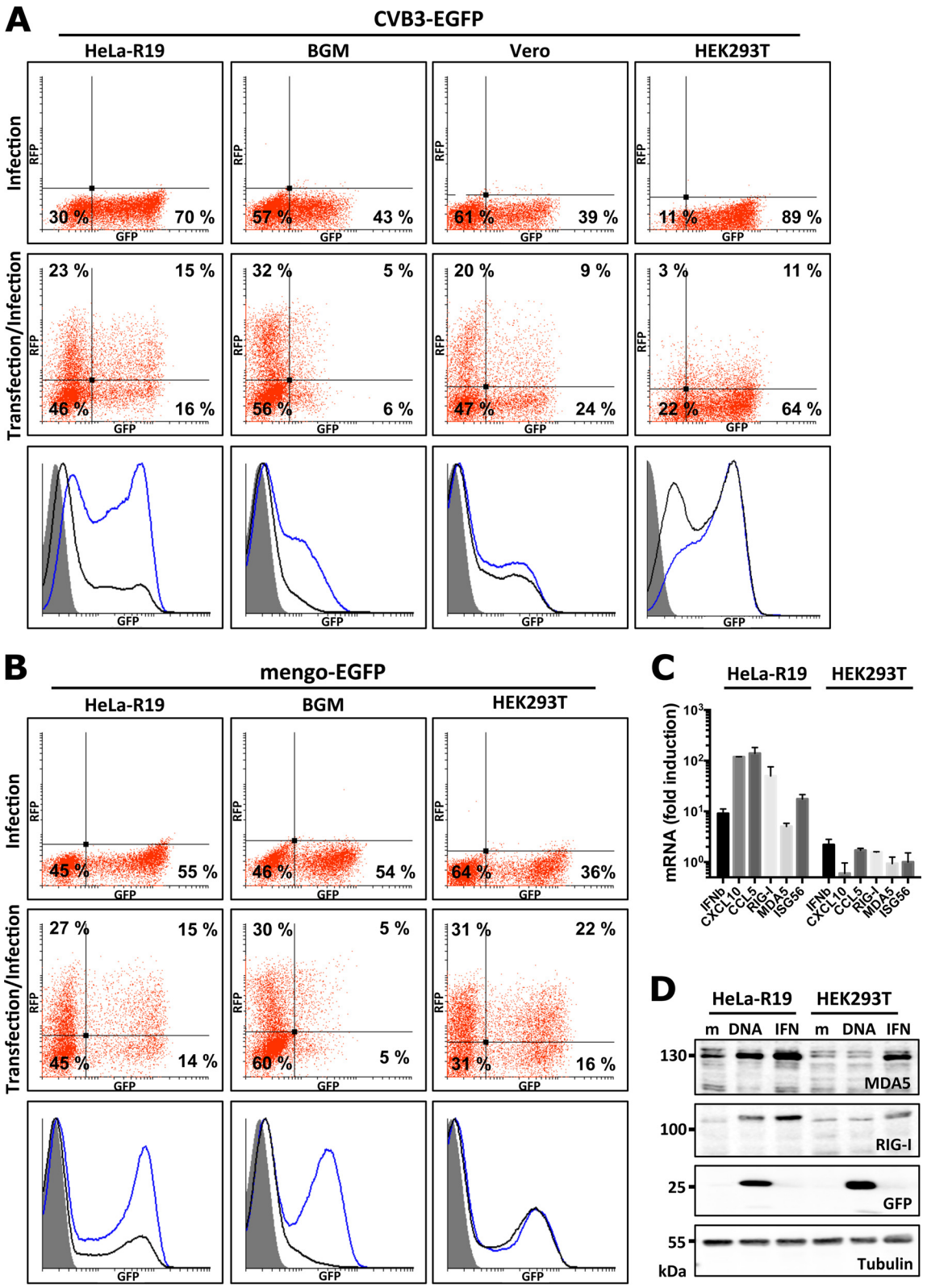

FIG 1 Plasmid DNA transfection restricts virus infection efficiency. (A) Flow cytometry analysis of CVB3-EGFP (coxsackievirus strain B3 EGFP reporter virus [13])-infected HeLa-R19, BGM, Vero-E6, and HEK293T cells. (Top) Scatter plots of GFP expression levels (*x* axis) and RFP expression levels (*y* axis) in mock-treated and CVB3-EGFP-infected cells. (Middle) Scatter plots of GFP expression levels (*x* axis) and RFP expression levels (*y* axis) in pcDNA-RFP-transfected and subsequently CVB3-EGFP-infected cells. (Bottom) Histograms of GFP expression levels in mock-treated cells (gray filled histogram), mock-treated and CVB3-EGFP-infected cells (blue line), and pcDNA-RFP-transfected and subsequently CVB3-EGFP-infected cells (black line). (B) Flow cytometry analysis of mengo-EGFP (mengovirus-EGFP reporter virus)-infected HeLa-R19, BGM, and HEK293T cells, as described for panel A. (C) RT-qPCR analysis of cytokine and ISG mRNA transcription after plasmid DNA transfection. Total RNA from mock-treated and plasmid DNA-transfected cells was isolated and used for RT-qPCR analysis of RIG-I, MDA5, and ISG56 mRNA levels. Fold induction values, corrected for actin mRNA levels, compared to mock-treated cells are shown. (D) Western blot analysis of protein levels. Lysates of mock-treated (m), pcDNA-GFP-transfected (DNA), and IFN-α-treated (IFN) cells were made and analyzed for expression of MDA5, RIG-I, and GFP. Additionally, detection of tubulin expression was used as a loading control.

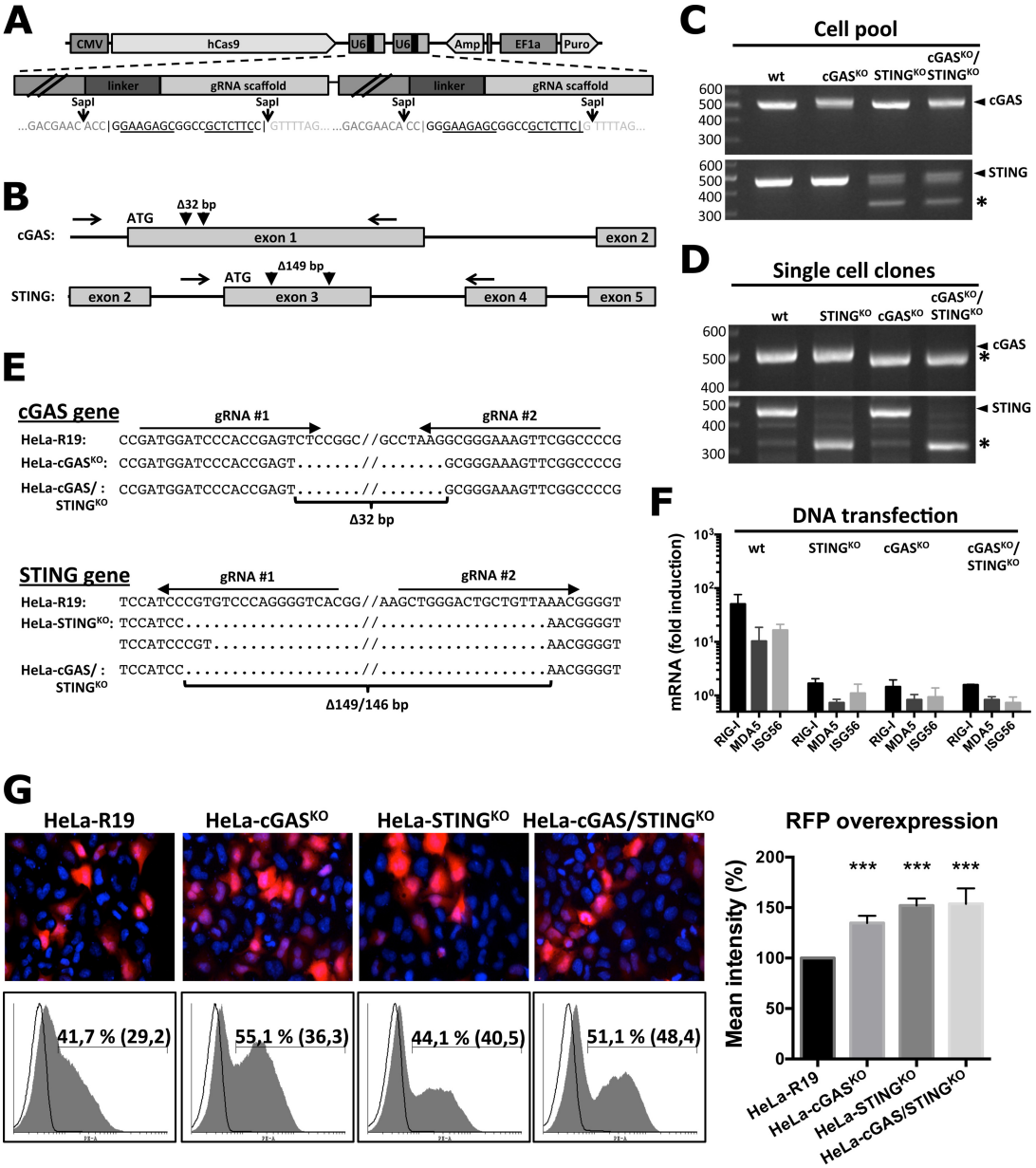

FIG 2 Characterization of the cGAS- and STING-knockout cells. (A) Linear representation of the pCRISPR-hCas9-2xgRNA-Puro plasmid. The human codon-optimized Cas9 gene (hCas9) possessing a nuclear localization sequence is expressed under the control of the cytomegalovirus (CMV) promoter (from pcDNA3.3-TOPO-hCas9 plasmid). The puromycin selection marker is expressed under the control of the EF1a promoter, and the two gRNA sequences, which are inserted as oligonucleotide duplexes into the nonpalindromic SapI sites using a four-fragment ligation, are expressed under the control of the U6 promoter (from the pSicoR-CRISPR-Cas plasmid). Gene-specific gRNA sequences can be introduced by replacing the linker sequences between the SapI recognition sequences. (B) Schematic representation of the gRNA target sequences in the cGAS gene (top) and STING gene (bottom). Arrowheads indicate the Cas9 cleavage sites downstream of the translation initiation site (ATG). Arrows indicate PCR primers to assess cleavage efficiency. Note that in both cases deletion of a 32- or 149-bp fragment will result in a frameshift mutation. (C) Genomic DNA from mock-treated cells (wt), pCRISPR-hCas9-2xcGAS-Puro-transfected cells (cGAS^{KO}), pCRISPR-hCas9-2xSTING-Puro-transfected cells (STING^{KO}), or cotransfected cells (cGAS^{KO}/STING^{KO}) was used for PCR analysis of the cGAS and STING gene integrity using primers flanking the Cas9 target sites (as shown in panel B). Arrowheads indicate expected sizes of the PCR products of the intact gene, and the asterisk indicates the PCR product of a gene possessing the intended deletion. (D) PCR analysis of the cGAS and STING gene integrity of single-cell clones, as described for panel C. (E) Sequence analysis of HeLa-R19, HeLa-cGAS^{KO}, HeLa-STING^{KO}, and HeLa-cGAS/STING^{KO} single-cell clones. Both alleles of the cGAS gene in HeLa-cGAS^{KO} and HeLa-cGAS/STING^{KO} possessed a 32-bp deletion. The STING gene in the HeLa-STING^{KO} single-cell clone showed a 149- and a 146-bp deletion, while both alleles in HeLa-cGAS/STING^{KO} possessed a 149-bp deletion. (F) RT-qPCR analysis of ISG mRNA transcription after plasmid DNA transfection in HeLa-R19 (wt), HeLa-cGAS^{KO}, HeLa-STING^{KO}, and HeLa-cGAS/STING^{KO} single-cell clones. Total RNA from mock-treated and plasmid DNA-transfected cells was isolated and used for RT-qPCR analysis of RIG-I, MDA5, and ISG56 mRNA levels. Fold induction values, corrected for actin mRNA levels, compared to mock-treated cells are shown. (G) RFP expression levels in HeLa-R19, HeLa-cGAS^{KO}, HeLa-STING^{KO}, and HeLa-cGAS/STING^{KO} single-cell clones. Plasmid DNA transfection efficiencies were comparable in all cell lines as shown by immunofluorescence assay (top) and flow cytometry analysis (bottom). Histograms show RFP expression levels in mock-treated (black line) and pcDNA-RFP-transfected (gray filled histogram) cells. The percentage of RFP-positive cells is indicated, and the mean intensity of RFP signal is shown between brackets. Knockout of cGAS and/or STING increases the mean intensity of RFP signal significantly (right graph; unpaired *t* test; ***, significant difference; $P < 0.001$; averages from 4 independent experiments).

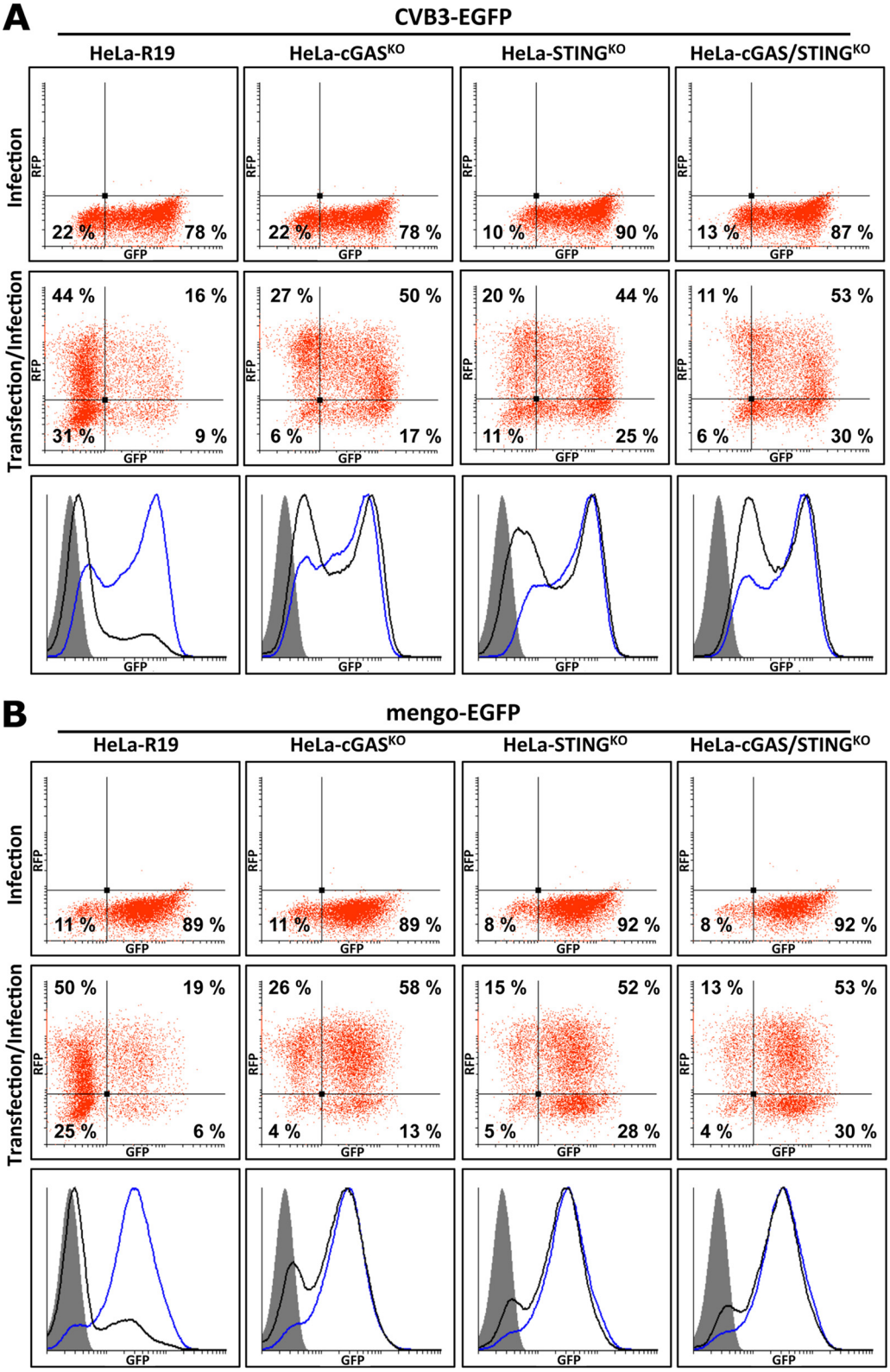

FIG 3 cGAS and STING knockout rescues plasmid DNA transfection-mediated virus restriction. (A) Flow cytometry analysis of CVB3-EGFP-infected HeLa-R19, HeLa-cGAS^{KO}, HeLa-STING^{KO}, and HeLa-cGAS/STING^{KO} cells. (Top) Scatter plots of GFP expression levels (*x* axis) and RFP expression levels (*y* axis) in mock-treated and CVB3-EGFP-infected cells. (Middle) Scatter plots of GFP expression levels (*x* axis) and RFP expression levels (*y* axis) in pcDNA-RFP-transfected and subsequently CVB3-EGFP-infected cells. (Bottom) Histograms of GFP expression levels in mock-treated cells (gray filled histogram), mock-treated and CVB3-EGFP-infected cells (blue line), and pcDNA-RFP-transfected and subsequently CVB3-EGFP-infected cells (black line). (B) Flow cytometry analysis of mengo-EGFP-infected HeLa-R19, HeLa-cGAS^{KO}, HeLa-STING^{KO}, and HeLa-cGAS/STING^{KO} cells, as described for panel A.

using PCR. Figure 2C shows that the cell pools possess the intended STING gene fragment deletion, while the cGAS gene fragment deletion was not clearly visible. From these cell pools, single-cell clones were generated by limiting dilution and again screened for gene fragment deletion. Sequence analysis of selected single-cell clone PCR products (Fig. 2D) confirmed the intended 32-bp (cGAS) and 149-bp (STING) deletions in both alleles (Fig. 2E). Sequence analysis of the HeLa-STING^{KO} single-cell clone PCR product resulted in two distinct sequence populations (Fig. 2E, bottom), which demonstrated that one allele possesses a 149-bp deletion and the other possesses a 146-bp deletion. To confirm that these knockout cells are also functional knockouts, we determined ISG mRNA transcription levels after plasmid DNA transfection. In line with our predictions, all knockout cells were deficient in plasmid DNA-induced ISG mRNA transcription (Fig. 2F). Interestingly, while analyzing plasmid DNA transfection efficiencies, which are comparable between cell lines, a significant increase in RFP main intensity was detected in knockout cells (Fig. 2G). This suggests that the lack of a plasmid DNA-induced antiviral state also increases transgene translation efficiency. In conclusion, we have used a one-plasmid CRISPR/Cas9 approach to generate cGAS/STING-knockout cells that are deficient in mounting an antiviral state of the cells following plasmid DNA transfection.

To investigate if cGAS/STING knockout rescues the infection efficiency of plasmid DNA-transfected cells, we again performed transfection/infection experiments. While plasmid DNA transfection in HeLa-R19 cells reduces CVB3-EGFP infection significantly (from 78% to 25%, comparable to the value shown in Fig. 1A), there was no apparent difference in infection efficiency in the knockout cells (from 78% to 67%, from 90% to 69%, and from 87 to 83%, respectively [Fig. 3A]). The mengo-EGFP infection efficiency of plasmid DNA-transfected cells was similarly increased in knockout cells (Fig. 3B). Thus, the data presented show that the plasmid DNA-induced activation of the cGAS/STING pathway, and the resulting antiviral state of the cells, is responsible for the poor infection efficiency. Moreover, we hereby present an easy and efficient CRISPR/Cas9 approach to overcome this problem. This approach is also applicable to other cell types and thus able to rescue virus infectivity after plasmid DNA transfection of other IFN-sensitive viruses.

ACKNOWLEDGMENTS

We are grateful to Robert Jan Lebbink from the University Medical Centre Utrecht for providing the pSicoR-CRISPR-Cas (11) plasmid. We obtained the pcDNA3.3-TOPO-hCas9 vector from the Church lab (12) via Addgene (Addgene plasmid 41815; hCas).

The work was supported by a Vici grant (NWO-918.12.628) from the Netherlands Organization for Scientific Research. Martijn A. Langereis is supported by a Veni grant (NWO-863.13.008), and Linda J. Visser is supported by a grant from the NWO-graduate program Infection and Immunity (NWO-022.004.018) from the Netherlands Organization for Scientific Research.

REFERENCES

1. **Chow J, Franz KM, Kagan JC.** 2015. PRRs are watching you: localization of innate sensing and signaling regulators. Virology **479–480:**104–109. http://dx.doi.org/10.1016/j.virol.2015.02.051.
2. **Schoggins JW, MacDuff DA, Imanaka N, Gainey MD, Shrestha B, Eitson JL, Mar KB, Richardson RB, Ratushny AV, Litvak V, Dabelic R, Manicassamy B, Aitchison JD, Aderem A, Elliott RM, García-Sastre A, Racaniello V, Snijder EJ, Yokoyama WM, Diamond MS, Virgin HW, Rice CM.** 2014. Pan-viral specificity of IFN-induced genes reveals new roles for cGAS in innate immunity. Nature **505:**691–695. http://dx.doi.org/10.1038/nature12862.
3. **Sun L, Wu J, Du F, Chen X, Chen ZJ.** 2013. Cyclic GMP-AMP synthase is a cytosolic DNA sensor that activates the type I interferon pathway. Science **339:**786–791. http://dx.doi.org/10.1126/science.1232458.
4. **Wu J, Sun L, Chen X, Du F, Shi H, Chen C, Chen ZJ.** 2013. Cyclic GMP-AMP is an endogenous second messenger in innate immune signaling by cytosolic DNA. Science **339:**826–830. http://dx.doi.org/10.1126/science.1229963.
5. **Ishikawa H, Barber GN.** 2008. STING is an endoplasmic reticulum adaptor that facilitates innate immune signalling. Nature **455:**674–678. http://dx.doi.org/10.1038/nature07317.
6. **Burdette DL, Monroe KM, Sotelo-Troha K, Iwig JS, Eckert B, Hyodo M, Hayakawa Y, Vance RE.** 2011. STING is a direct innate immune sensor of cyclic di-GMP. Nature **478:**515–518. http://dx.doi.org/10.1038/nature10429.
7. **Desmyter J, Melnick JL, Rawls WE.** 1968. Defectiveness of interferon production and of rubella virus interference in a line of African green monkey kidney cells (Vero). J Virol **2:**955–961.
8. **Marraffini LA, Sontheimer EJ.** 2010. CRISPR interference: RNA-directed adaptive immunity in bacteria and archaea. Nat Rev Genet **11:**181–190. http://dx.doi.org/10.1038/nrg2749.
9. **Cong L, Ran FA, Cox D, Lin S, Barretto R, Habib N, Hsu PD, Wu X, Jiang W, Marraffini LA, Zhang F.** 2013. Multiplex genome engineering using CRISPR/Cas systems. Science **339:**819–823. http://dx.doi.org/10.1126/science.1231143.
10. **Zheng Q, Cai X, Tan MH, Schaffert S, Arnold CP, Gong X, Chen C-Z, Huang S.** 2014. Precise gene deletion and replacement using the CRISPR/Cas9 system in human cells. Biotechniques **57:**115–124. http://dx.doi.org/10.2144/000114196.
11. **Van de Weijer ML, Bassik MC, Luteijn RD, Voorburg CM, Lohuis MAM, Kremmer E, Hoeben RC, LeProust EM, Chen S, Hoelen H, Ressing ME, Patena W, Weissman JS, McManus MT, Wiertz EJHJ, Lebbink RJ.** 2014. A high-coverage shRNA screen identifies TMEM129 as an E3 ligase involved in ER-associated protein degradation. Nat Commun **5:**3832. http://dx.doi.org/10.1038/ncomms4832.
12. **Mali P, Yang L, Esvelt KM, Aach J, Guell M, DiCarlo JE, Norville JE, Church GM.** 2013. RNA-guided human genome engineering via Cas9. Science **339:**823–826. http://dx.doi.org/10.1126/science.1232033.
13. **Lanke KHW, van der Schaar HM, Belov GA, Feng Q, Duijsings D, Jackson CL, Ehrenfeld E, van Kuppeveld FJM.** 2009. GBF1, a guanine nucleotide exchange factor for Arf, is crucial for coxsackievirus B3 RNA replication. J Virol **83:**11940–11949. http://dx.doi.org/10.1128/JVI.01244-09.